1 September 2001

ELSEVIER

Optics Communications 196 (2001) 221–228

OPTICS COMMUNICATIONS

www.elsevier.com/locate/optcom

Superradiant amplification from two coupled optically dense two-level slabs

Jamal T. Manassah [a,*], Irina Gladkova [b]

[a] HMS Technology Corporation, P.O. Box 592, New York, NY 10028-0005, USA
[b] Department of Computer Science, City College of New York, New York, NY 10031, USA

Received 25 April 2001; received in revised form 1 June 2001; accepted 21 June 2001

Abstract

We study a system consisting of two coupled optically dense slabs with the same resonant atoms but initially having different degrees of inversion. We show that it is possible to modify the superradiant amplification characteristics of this system by varying the distance between slabs; in particular, we show that the burst intensity, delay and width are periodic functions of this distance with period equal to $\lambda/2$. This feature and others of the emitted radiation can be explained by noting that a slab with resonant atoms in the ground state acts on the macroscopic level as a strong absorber and therefore also as a reflector of incident radiation resonant with its active atoms.

Keywords: Superradiance; Coupled quantum systems; Pressure-induced resonators; Optically dense material

1. Introduction

The large value of the reflectivity at every point along the propagation path of a signal, in an optically dense resonant two-level medium (i.e. $\alpha\lambda < 1$), necessitates that both the forward and backward waves be included in the analysis of Maxwell equations in this medium. The simultaneous presence of the forward and backward waves results into situations where resonator-like standing waves can develop in the sample without the need for end mirrors; this situation can be realized when the pressure broadening in a gas substantially exceeds the Doppler broadening, hence the name ''pressure-induced resonators''.

Previously, we have shown [1–4] that, in the superradiant regime [5], an inverted system of such resonant atoms radiates optimally when in a given standing-wave-like pattern. The atomic polarization and the total field are eigenfunctions of the spatial inversion operator with respect to the center of the slab, for sample's length in, what we called the symmetric sectors. An asymmetric transition domain separates two consecutive symmetric sectors having opposite parity eigenvalues. In the symmetric sectors, the electromagnetic field spatial distributions are similar to those found in a slab resonant cavity, and the forward and backward emission fluxes are equal; while, in the transition domains, the forward and backward emissions are not equal.

* Corresponding author. Fax: +1-212-650-7185.
E-mail address: manassah@ees1s0.engr.ccny.cuny.edu (J.T. Manassah).

0030-4018/01/$ - see front matter
PII: S0030-4018(01)01387-6

In this paper, we consider a system essentially consisting of two slabs doped with the same resonant atoms and study the effect of their coupling on the superradiant amplification. In particular, we investigate the dependence of the system's superradiance emission on the distance between two slabs having the same resonant material but which initially have different degrees of population inversion. We show that the superradiant radiation intensity, delay and temporal width are periodic functions of the distance between the two slabs. Macroscopically, these results are shown to be a consequence of whether a standing-wave configuration of the field develops in the region between the two slabs.

We solve the above problem numerically by integrating the Maxwell–Bloch integro-differential coupled equations describing the two-slab system.

We were motivated in conducting the present study by our desire:

1. To satisfactorily analyze the interesting problem of superradiant emission from a system consisting of two subsystems that are physically separated but coupled through the radiation field, in particular whether any coherence develops between the subsystems; and
2. To develop the necessary computational tools for the consideration of teleporting of an unknown collective internal state from one atomic ensemble to another only using coherent light and under conditions when the quantum jumps of individual atoms have negligible effect on the dynamics of collective operators [6].

2. Maxwell–Bloch equations

The physical system that we analyze here is that of a passive dielectric medium doped with active atoms. We consider, specifically the geometry whereby the sample's doping profile is approximated by three distinct zones. The first and third zones are heavily doped, while in the second (middle) zone the density of the doping atoms is zero (see Fig. 1).

In this atomic/dielectric medium system, the total polarization consists of the sum of the linear

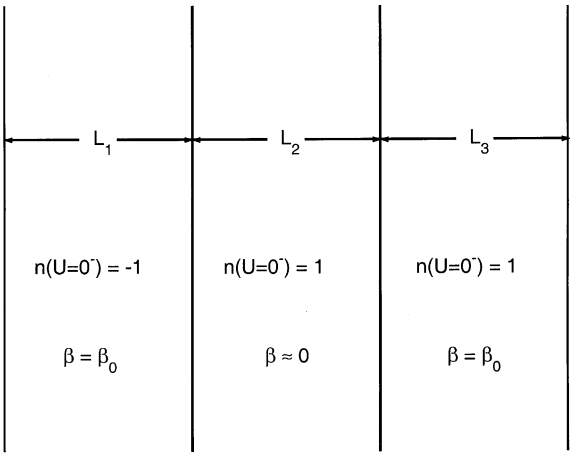

Fig. 1. System's initial configuration.

polarization due to the embedding dielectric medium plus the resonant polarization due to the two-level atomic system:

$$P = P_{\mathrm{NR}} + P_{\mathrm{R}} \tag{1}$$

The linear polarization P_{NR} (where the subscript NR stands for non-resonant, and R for resonant) is given by:

$$P_{\mathrm{NR}} = \alpha\varepsilon_0 E_{\mathrm{L}} \tag{2}$$

where α is the medium linear susceptibility, and the local (Lorentz) field E_{L} is given by [7]:

$$E_{\mathrm{L}} = E + P/3\varepsilon_0 \tag{3}$$

and where E is the Maxwell (macroscopic) field.

Using Eqs. (1)–(3), the total polarization can be written as:

$$P = \frac{\alpha\varepsilon_0 E}{1 - \frac{1}{3}\alpha} + \frac{P_{\mathrm{R}}}{1 - \frac{1}{3}\alpha} \tag{4}$$

where P_{R} is obtained from Bloch equations, evaluated with the local field, and not the Maxwell field.

Expressed in the above variables, the Clausius–Mosotti equation takes the form:

$$\varepsilon_{\mathrm{r}} = n_{\mathrm{r}}^2 = \frac{1 + 2\alpha/3}{1 - \alpha/3} \tag{5}$$

where n_r, the passive dielectric's index of refraction, is assumed here to be real. (The Kramer–Kronig relations, derived only on the assumption of causality, require that $\mathrm{Im}(n_r) \neq 0$, however, we will work in the spectral regime where this contribution can be neglected over the propagation lengths under consideration.)

The dynamics of the interaction of the electromagnetic field with the ensemble of active two-level atom system is described by Bloch equations. If we neglect the counter-rotating term in the Hamiltonian, i.e. replacing the electromagnetic real field $(E\mathrm{e}^{-\mathrm{i}\omega_c t} + E^*\mathrm{e}^{+\mathrm{i}\omega_c t})$ by $E\mathrm{e}^{-\mathrm{i}\omega_c t}$, where ω_c is the carrier frequency, Bloch equations reduce to:

$$\frac{\partial\chi}{\partial U} = -\left[\mathrm{i}\left[\left(\overline{\Omega}_0 - \overline{\Omega}_c\right) + \overline{\Delta}\right] + \bar{\gamma}_2\right]\chi + \frac{\mathrm{i}n\phi_L}{2} \tag{6}$$

$$\frac{\partial n}{\partial U} = -\mathrm{i}\left[\chi^*\phi_L - \chi\phi_L^*\right] + \bar{\gamma}_1(1-n) \tag{7}$$

where we are normalizing the dynamical variables and coordinates as follows:

$$\phi = \frac{dET_2^*}{\hbar}; \quad \chi = \frac{p}{d}; \quad U = \frac{t}{T_2^*}; \quad \overline{\Delta} = \Delta T_2^*;$$
$$\bar{\gamma}_{(1,2)} = \gamma_{(1,2)}T_2^*; \quad \overline{\Omega}_{(0,c)} = \omega_{(0,c)}T_2^*$$

p is the x–y components of the Bloch vector, $p = p_x + \mathrm{i}p_y$, n is the population difference between the ground and excited states, ω_0 is the active atom resonant frequency, γ_1 and γ_2 are the longitudinal and transverse decay rates, d is the atomic transition dipole moment, T_2^* is the inhomogeneous dephasing time, and Δ is the detuning of a particular group of atoms in the ensemble from the single atom resonant frequency. The normalized local field ϕ_L is given by:

$$\phi_L = \frac{1}{\left(1 - \frac{1}{3}\alpha\right)}\phi + \frac{8\beta}{3\left(1 - \frac{1}{3}\alpha\right)}\chi \tag{8}$$

where $\beta(\bar{z}) = \rho(\bar{z})d^2T_2^*/8\hbar\varepsilon_0$ and $\rho(\bar{z})$ is the spatially dependent active atom number density. The normalized Lorentz shift [8,9], neglecting quantum corrections originating from the scattering amplitude due to collision between atoms and that are present in a gaseous medium, is then given for low excitation by $4\beta/3(1-\alpha/3)$.

The transverse relaxation decay rate consists of three components. The first component is equal to half the longitudinal relaxation constant. The second contribution is due to the short range dipole–dipole interaction [8,9] (which is very important here since the active atoms density is high in an optically dense medium). The third contribution is due to the interaction of the active atoms with the different quantum modes of the dielectric medium, and which may be controlled by cooling the dielectric medium. Specifically:

$$\bar{\gamma}_2 = \frac{\bar{\gamma}_1}{2} + (1.16)(1.15)\left(\frac{2\pi}{3n_r^2}\right)\beta + \bar{\gamma}_T \tag{9}$$

The second term of Eq. (9) has an additional factor of 1.16 to that of the standard gas pressure-broadened expression for the line width. It corresponds to the off-the-mass shell correction to the scattering amplitude, which quantity should be used in the computation of the atomic self-energy when the active atoms are immobile and embedded in a dielectric. This is equivalent, as was shown in Ref. [9], to using the statistical theory results in computing the spectral broadening of the excited state due to the dipole–dipole interaction between an excited and a ground state atom.

Maxwell wave equation is given by:

$$\frac{\partial^2\phi}{\partial\bar{z}^2} - \varsigma^2\frac{\partial^2\phi}{\partial U^2} = \frac{8\beta\varsigma^2}{(1+2\alpha/3)}\left\langle\frac{\partial^2\chi}{\partial U^2}\right\rangle_{\overline{\Delta}} \tag{10}$$

where $\bar{z} = (\omega_c n_r/c)z$, $\varsigma = 1/\omega_c T_2^*$, and $\langle\chi\rangle_{\Delta}$ represents the normalized polarizability averaged over the inhomogeneous distribution, assumed here Gaussian, and given by:

$$g(\overline{\Delta}) = \frac{1}{\sqrt{2\pi}}\exp\left(-\frac{\overline{\Delta}^2}{2}\right) \tag{11}$$

To avoid the usual difficulties associated with solving a second order differential equation (Eq. (10)) when the forward and backward waves are comparable in magnitude, we replace it by its equivalent integral equation form [10–12]:

$$\phi(\bar{z}, U) = \phi_{in}(\bar{z}=0, U_{ret})\exp(\mathrm{i}\bar{z}) + \mathrm{i}\frac{4}{(1+2\alpha/3)} \times \int_0^{\bar{L}}\beta(\bar{z}')\exp(\mathrm{i}|\bar{z}-\bar{z}'|)\langle\chi(\bar{z}', U_{ret}, \overline{\Delta})\rangle_{\Delta}\mathrm{d}\bar{z}' \tag{12}$$

where $\overline{L}$ is the normalized sample length, and the retarded normalized time is given, such that the space–time doublet is defined as follows:

$$(\bar{z}, U_{\text{ret}}) = (\bar{z}, U - \varsigma\bar{z}) \tag{13}$$

The mixed boundary and initial conditions for the problem are:

$$\phi_{\text{in}}(\bar{z} = 0, U) = \phi_{\text{in}}^{0} \exp\left(- \frac{U^2}{(\tau/T_2^*)^2} \right) \tag{14}$$

where $\phi_{\text{in}}^{0} = \Sigma T_2^*/(\sqrt{\pi}\tau)$, and Σ is the incoming pulse area; and

$$\chi(\bar{z}, U = 0^-, \Delta) = 0 \tag{15}$$

$$\begin{aligned} &n(0 < \bar{z} \leqslant \overline{L}_1, U = 0^-, \Delta) = -1 \\ &n(\overline{L}_1 < \bar{z} \leqslant \overline{L}_1 + \overline{L}_2 + \overline{L}_3, U = 0^-, \Delta\ ) = 1 \end{aligned} \tag{16}$$

for $\bar{z} > 0$. ($U = 0^-$ refers to the time prior to the incident external signal being switched-on.)

The doping profile is given by:

$$\begin{aligned} &\beta(0 < \bar{z} \leqslant \overline{L}_1) = \beta_0 \\ &\beta(\overline{L}_1 < \bar{z} < \overline{L}_1 + \overline{L}_2) = 0 \\ &\beta(\overline{L}_1 + \overline{L}_2 \leqslant \bar{z} < \overline{L}_1 + \overline{L}_2 + \overline{L}_3) = \beta_0 \end{aligned} \tag{17}$$

To mimic the electromagnetic field vacuum fluctuations, we introduce an incoming pulse from the left which duration is longer than any of the relaxation times of the atomic system and which area is equal to the rms of the field zero modes.

For the clarity of the subsequent presentation, we refer to the radiation emitted to the right as the transmitted radiation, and that to the left as the reflected radiation.

3. Results

To illustrate the substantial effects that the distance of the second slab from the first slab can have on the field spatio-temporal profile, we plot in Fig. 2 this quantity for the cases that the distance between the slabs is equal respectively to 5.25λ and 5.75λ. The active atom density in the two slabs is taken to be the same. The first slab's length is chosen so that in isolation its emission pattern is typical of those belonging to what we defined in Refs. [1–3] as a symmetric sector, i.e. the transmitted and the reflected radiation profiles are the same in every detail. Furthermore, the length of the second slab is taken to be equal to that of the first slab.

Examining the results from the above figures, and comparing them to each other and to those from an isolated slab, we note that:

1. For a distance between the slabs equal to a multiple of $\lambda/2$, the total reflected radiation flux increased, as compared with the isolated slab, and the position of the main peak and the width of its temporal profile decreased.
2. For the distance between the slabs equal to 5.75λ, the total reflected signal flux is smaller, the delay in the position of the main peak is longer and the width of the temporal profile is larger than the corresponding quantities for the isolated slab.
3. The presence of the second slab greatly reduces the transmitted signal, thus acting as absorber with the resonant atoms near the closer surface of the second slab being inverted.
4. The field's amplitude follows Beer's law in the region close to the second slab's face farthest away from the first slab. This is a consequence of having the length of the second slab being equal to that of the first slab and therefore limiting the degree to which the second slab can be saturated by the radiation initially emitted from the first slab. (At most half the flux is emitted to the right and thus, under the present conditions, exciting at most half the atoms of the second slab.)
5. A standing-wave pattern in the field distribution develops in the region between the two slabs' closest faces, for the case that the separation between the slabs is a multiple of $\lambda/2$. This implies that there are different phase relations between the direct backward field emitted from the atoms of the first slab and the signal reflected from the second slab in the two cases considered.
6. In addition to the main peak in the output field temporal profile, secondary peaks develop as a result of the Burnham–Chiao oscillations [13].

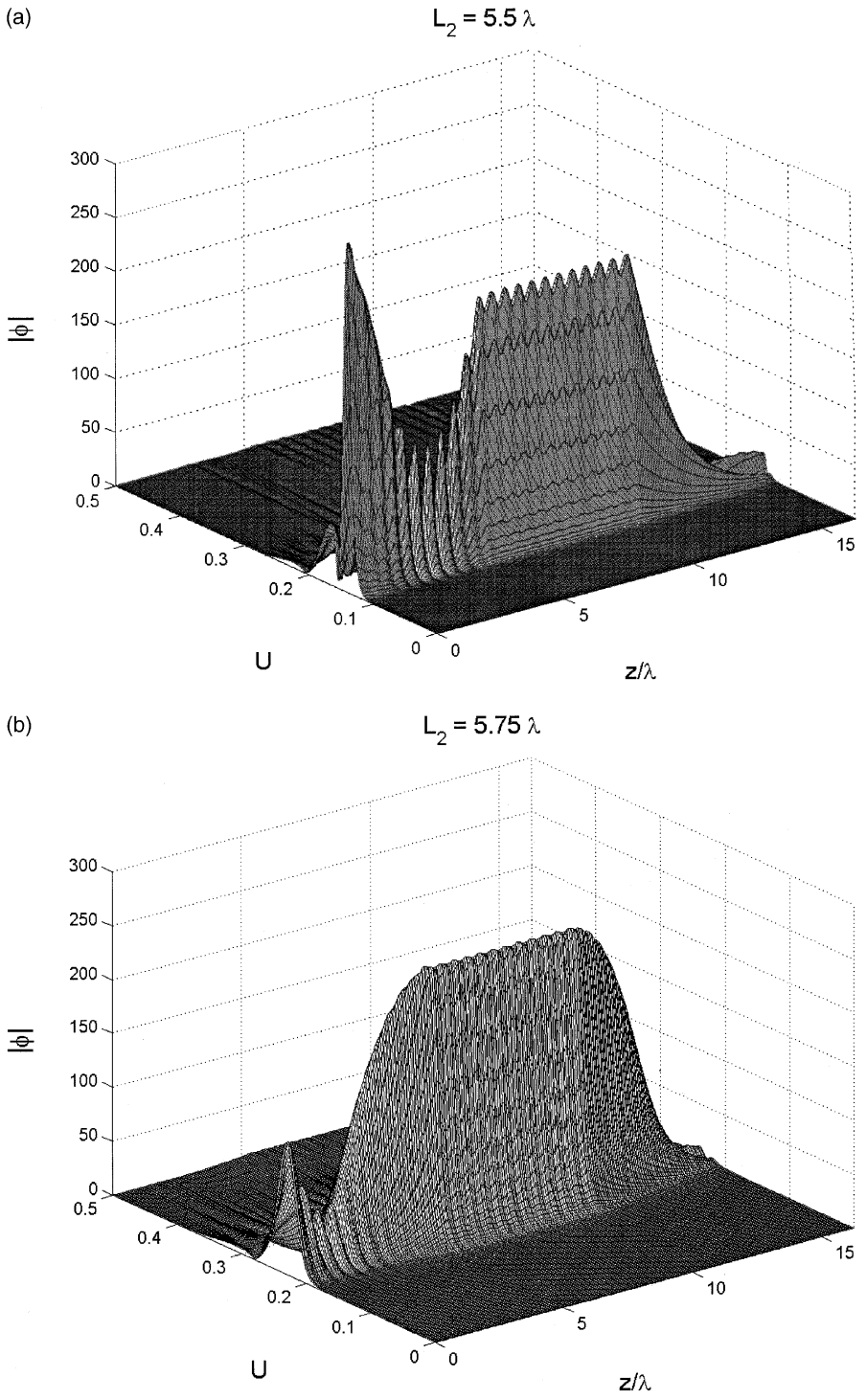

Fig. 2. The spatio-temporal 3D plot of the magnitude of the normalized field. (a) $L_1 = 5.25\lambda$; $L_2 = 5.50\lambda$; $L_3 = 5.25\lambda$, $\beta_0 = 10$; $n_r = 1$; $\bar{\gamma}_1 = 1/26$; $\bar{\gamma}_T = 0$, (b) $L_1 = 5.25\lambda$; $L_2 = 5.75\lambda$; $L_3 = 5.25\lambda$, $\beta_0 = 10$; $n_r = 1$; $\bar{\gamma}_1 = 1/26$; $\bar{\gamma}_T = 0$.

Having observed in the previous figure clear macroscopic features that strongly suggest that the second slab acts as a partially reflecting mirror, we should test the quantitative validity of this hypothesis by investigating the emission from the system if the distance L_2 between the two slabs is varied. We would expect that, if the above physical picture is valid, due to the result that the field emitted by a planar sheet of dipoles in phase is a plane wave, to obtain periodic functions in the distance between the slabs for the different quantities specifying the reflected radiation.

We plot the different characteristics of the reflected radiation, in Fig. 3, on the interval $5.25\lambda \leqslant L_2 \leqslant 6.25\lambda$; under the previous conditions of equal slab length and having the atoms of the left slab totally inverted while the second slab has originally all its atoms in the ground state. These figures summarize the main result of this paper: all the functions characterizing the reflected signal are periodic and have, as they should, period $\lambda/2$. (We verified numerically this periodicity for distances between the slabs extending up to 100λ.) Furthermore, we expect this periodicity to continue to hold true, as long as the time for the light to travel back and forth from the first slab to the second slab is substantially shorter than the delay time of the superradiance main peak, where the above quasi-stationary analysis remains valid.

So far, and in all the above cases studied, we assumed that the length of the second slab was equal to that of the first slab. Next, we would like to examine what happens to the fluxes when the length of the second slab is smaller than that of the first.

We plot in Fig. 4, the flux and the delay of the main peak of the reflected signal, and in Fig. 5, the

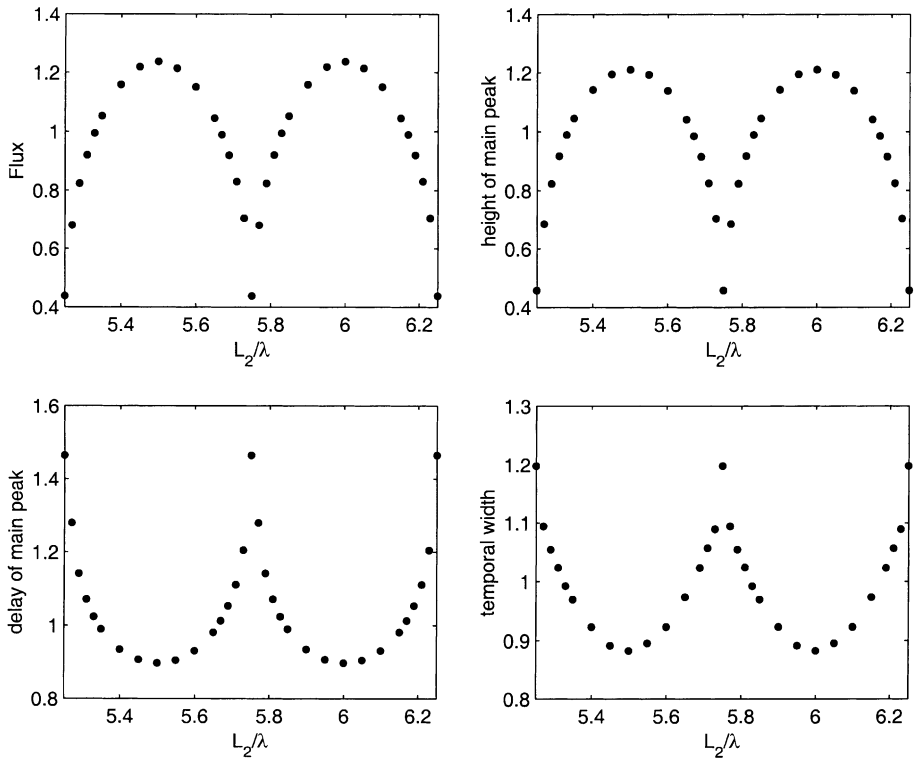

Fig. 3. The reflected field (i.e. at $z = 0$) characteristics are plotted as a function of L_2. (The results are normalized to those of the single slab with $L_1 = L = 5.25\lambda$.) $L_1 = 5.25\lambda$; $L_3 = 5.25\lambda$; $\beta_0 = 10$; $n_r = 1$; $\bar{\gamma}_1 = 1/26$; $\bar{\gamma}_T = 0$. (a) Flux; (b) main peak height; (c) main peak delay; (d) width of the temporal profile of $|\phi(\bar{z} = 0, U)|^2$.

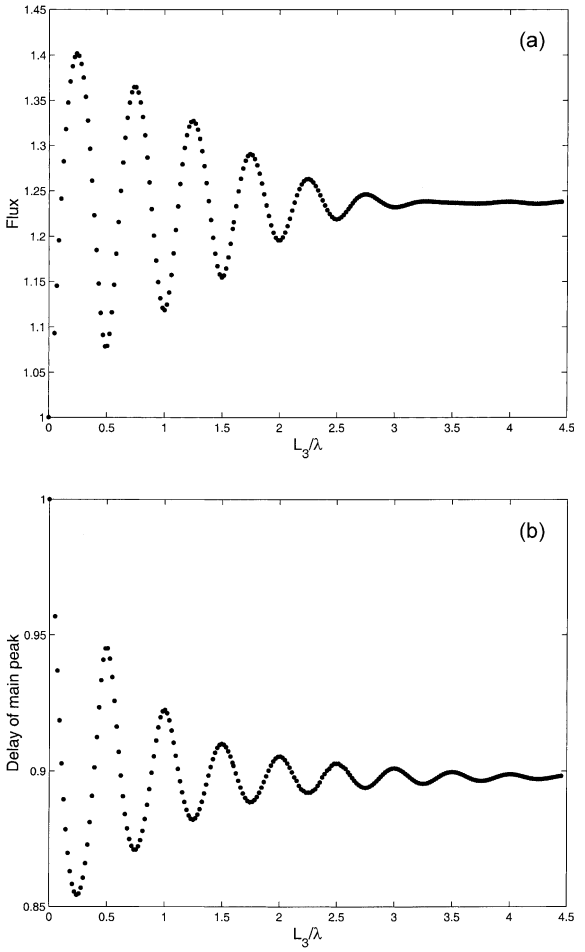

Fig. 4. The reflected field characteristics are plotted as a function of L_3. (The results are normalized to those of the single slab with $L_1 = L = 5.25\lambda$.) $L_1 = 5.25\lambda$; $L_2 = 5.50\lambda$; $\beta_0 = 10$; $n_r = 1$; $\bar{\gamma}_1 = 1/26$; $\bar{\gamma}_T = 0$. (a) Flux; (b) main peak delay.

flux of the transmitted signal as function of L_3, the length of the second slab. We note that the envelope of each of the outgoing radiation fluxes approaches respectively, for large L_3, the asymptotic value corresponding to the result when the second slab length is equal to the length of the first slab. On the other hand, we observe that, for smaller values of L_3, the values of both outgoing fluxes are modulated by a periodic function with period $\lambda/2$, and the amplitude of these modulations is decreasing with an increase in the value of L_3.

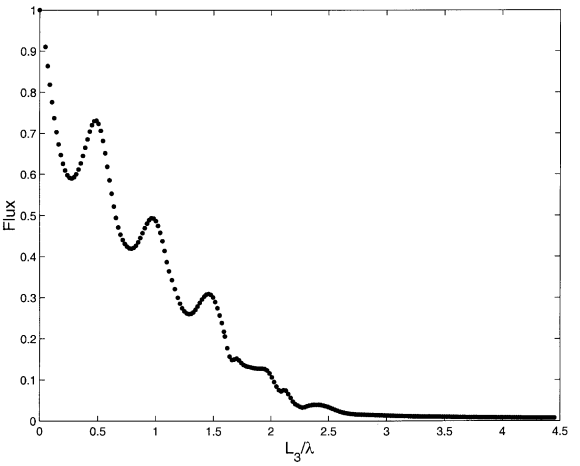

Fig. 5. The transmitted field flux is plotted as a function of L_3. (The results are normalized to those of the single slab with $L_1 = L = 5.25\lambda$.) (Same parameters as those of Fig. 4.)

4. Conclusion

In this paper, we investigated superradiant amplification from a system consisting of essentially two optically dense slabs doped with two-level resonant atoms and that are separated by a region of zero doping. We showed that, if the two slabs are of equal length, and that if initially one of the slabs has all its atoms inverted, while, in the other slab, the active atoms are all in the ground state, then the superradiant burst intensity, the delay of the main peak and the width of the field's temporal profile are all periodic functions of the length of the inert region between the slabs with period $\lambda/2$. In summary, the maximum reflected flux is obtained when a standing-wave configuration in the region between the two slabs is achieved.

References

[1] J.T. Manassah, B. Gross, Opt. Commun. 143 (1997) 329.
[2] J.T. Manassah, B. Gross, Opt. Exp. 1 (1997) 141.
[3] J.T. Manassah, B. Gross, Opt. Commun. 155 (1998) 213.
[4] J.T. Manassah, I. Gladkova, Opt. Commun. 189 (2001) 87.
[5] R.H. Dicke, Phys. Rev. 93 (1954) 99.
[6] L.M. Duan, J.I. Cirac, P. Zoller, E.S. Polzik, Phys. Rev. Lett. 85 (2000) 5643.

[7] H.A. Lorentz, The Theory of Electrons, Dover, New York, 1952.
[8] R. Friedberg, S.R. Hartmann, J.T. Manassah, Phys. Rep. C 7 (1973) 101.
[9] J.T. Manassah, Phys. Rep. 101 (1983) 359.
[10] V. Malyshev, E.C. Jarque, J. Opt. Soc. Am. 12 (1995) 1868.
[11] M.G. Benedict, E.D. Trifonov, Phys. Rev. 38 (1988) 2854.
[12] M.G. Benedict, V.A. Malyshev, E.D. Trifonov, I. Zaitsev, Phys. Rev. 43 (1991) 3854.
[13] D.C. Burnham, R.Y. Chiao, Phys. Rev. 188 (1969) 667.